Experimental Demonstration of the Lower Leg Trajectory Error Framework Using Physiological Data as Inputs

Kathryn M. Olesnavage
GEAR Laboratory,
Department of Mechanical Engineering,
Massachusetts Institute of Technology,
Cambridge, MA 02139
e-mail: kolesnav@mit.edu

Victor Prost[1]
GEAR Laboratory,
Department of Mechanical Engineering,
Massachusetts Institute of Technology,
Cambridge, MA 02139
e-mail: vprost@mit.edu

William Brett Johnson
GEAR Laboratory,
Department of Mechanical Engineering,
Massachusetts Institute of Technology,
Cambridge, MA 02139
e-mail: wbj@mit.edu

Matthew J. Major
Jesse Brown VA Medical Center,
Department of Physical Medicine and Rehabilitation,
Northwestern University,
Chicago, IL 60208
e-mail: matthew-major@northwestern.edu

Amos G. Winter, V
GEAR Laboratory,
Department of Mechanical Engineering,
Massachusetts Institute of Technology,
Cambridge, MA 02139
e-mail: awinter@mit.edu

Experimental Demonstration of the Lower Leg Trajectory Error Framework Using Physiological Data as Inputs

While many studies have attempted to characterize the mechanical behavior of passive prosthetic feet to understand their influence on amputee gait, the relationship between mechanical design and biomechanical performance has not yet been fully articulated from a fundamental physics perspective. A novel framework, called lower leg trajectory error (LLTE) framework, presents a means of quantitatively optimizing the constitutive model of prosthetic feet to match a reference kinematic and kinetic dataset. This framework can be used to predict the required stiffness and geometry of a prosthesis to yield a desired biomechanical response. A passive prototype foot with adjustable ankle stiffness was tested by a unilateral transtibial amputee to evaluate this framework. The foot condition with LLTE-optimal ankle stiffness enabled the user to replicate the physiological target dataset within 16% root-mean-square (RMS) error. Specifically, the measured kinematic variables matched the target kinematics within 4% RMS error. Testing a range of ankle stiffness conditions from 1.5 to 24.4 N·m/deg with the same user indicated that conditions with lower LLTE values deviated the least from the target kinematic data. Across all conditions, the framework predicted the horizontal/vertical position, and angular orientation of the lower leg during midstance within 1.0 cm, 0.3 cm, and 1.5 deg, respectively. This initial testing suggests that prosthetic feet designed with low LLTE values could offer benefits to users. The LLTE framework is agnostic to specific foot designs and kinematic/kinetic user targets, and could be used to design and customize prosthetic feet. [DOI: 10.1115/1.4048643]

1 Introduction

Many studies have shown that the mechanical characteristics of a prosthetic foot affect a user's gait mechanics [1–9], but it is not yet understood exactly how the mechanical design of a foot affects its functionality [10]. Without this knowledge, prosthetic feet cannot be designed to achieve optimal performance deterministically; they must instead be designed empirically through trial and error. Correlating mechanical characteristics, sometimes referred to as Amputee Independent Prosthesis Properties [11], to biomechanical functionality has consequently been the focus of many studies [7,8,12–14].

Approaches to the mechanical characterization of prosthetic feet can be separated into one of two categories: (1) lumped parameter models and (2) roll-over models [14]. Lumped parameter models use discrete viscoelastic properties, such as stiffness and damping, to represent the behavior of a prosthetic foot. Such studies often simplify the mechanical behavior of a foot to linear models of the forefoot [15–18], heel [19,20], or both [5,21], using a single-load orientation for each. The spring-damper models employed by these lumped parameter representations provide a rapid means to measure and compare the mechanical properties of prosthetic feet. However, these simple models have typically only described the response of the foot under particular loading scenarios. Consequently, they do not adequately describe the behavior of a prosthetic foot throughout stance phase, nor is there a consensus on which lumped parameters are most important or how they are connected to biomechanical functionality apart from a few intuitive trends, such as increasing the compliance of the forefoot increases a foot's range of motion [3,22]. Only recently have the viscoelastic torque-angle properties of a biological foot/ankle complex been measured [23], enabling them to be incorporated into a quasi-passive prosthetic foot design [24]. Without a quantitative, predictive relationship between lumped parameter models and walking behavior, desirable values for the lumped parameters are difficult to determine. Therefore, lumped parameter models as they have been investigated in prior work cannot be used as design objectives by themselves.

Roll-over geometries provide a more comprehensive depiction of the mechanical behavior of a prosthetic foot than lumped parameter models. The roll-over geometry of a foot is defined as the path of the center of pressure (CoP) along the bottom of the foot throughout the course of a step, depicted in the shank reference frame [25,26]. Because roll-over geometries can be measured through benchtop mechanical tests and motion analysis of human subjects [13,25,27–29], they provide a relation between the mechanical design of a prosthetic foot and its biomechanical performance. Several studies have suggested that prosthetic feet with roll-over geometries similar to typical physiological roll-over geometries result in benefits such as reduced metabolic cost of walking [30,31], more symmetric gait [25], and reduced total joint moment and joint power costs [32]. However, while roll-over geometries provide a more complete representation of a prosthetic foot than most lumped parameter models, they do not sufficiently

[1]Corresponding author.

Manuscript received November 29, 2019; final manuscript received September 10, 2020; published online December 10, 2020. Assoc. Editor: Sara Wilson.

describe the mechanical functionality of a prosthetic foot; roll-over geometry does not include any information about the orientation of the shank reference frame with respect to the global reference frame. In previous work, the authors have demonstrated that two different prosthetic feet with identical roll-over geometries can result in very different gait kinematics, even under the same ground reaction forces (GRFs) [33,34]. Consequently, roll-over geometry is insufficient to be used as a design objective for prosthetic feet.

The authors have introduced a novel framework for prosthetic foot design, in which a constitutive model of a foot is optimized to most closely connect a reference lower leg trajectory to a reference kinetic dataset [34]. A cost function, called the lower leg trajectory error (LLTE), is calculated to evaluate how close the computed prosthetic side lower leg trajectory is to a reference set of target lower leg kinematic data. The LLTE framework provides a quantitative, deterministic means of connecting the mechanical design of a prosthetic foot to its biomechanical functionality, and enables the optimization of a foot design (stiffness and geometry) to yield a desired biomechanical response. Previous work by the authors demonstrated this method conceptually by optimizing three different simple prosthetic foot models, each with two degrees-of-freedom [34]. The aims of this paper are to:

(1) quantify the accuracy of the constitutive model behind the LLTE framework, whereby lower leg kinematics can be predicted given the ground reaction forces acting on a prosthetic foot of known stiffness and geometry;
(2) investigate the extent to which a foot design optimized with the LLTE framework can replicate the reference kinematics and kinetics that were used as inputs to the framework (in this case, physiological values); and
(3) explore the sensitivity of the optimized design (and constitutive model) and evaluate how variations in foot stiffness affect walking performance.

1.1 Lower Leg Trajectory Error Framework. The Lower Leg Trajectory Error framework requires a reference dataset of GRF inputs and target kinematic outputs to calculate the LLTE value for a given prosthetic foot with known mechanical behavior. The framework consists of applying the reference set of horizontal and vertical GRFs (GRF_x and GRF_y, respectively) to the constitutive model of a foot at locations defined by the corresponding CoP data, x_{cp}. Each of these variables, GRF_x, GRF_y, and x_{cp}, are functions of time spanning the stance phase. The deformed shape of the foot in response to the reference loading at each time-step is calculated quasi-statically using its constitutive behavior, which is governed by the foot's stiffness and geometry. This deformation can be calculated using fundamental physics for simple prosthetic foot designs, or finite element analysis for more complicated designs. By assuming a no-slip condition between the foot and the ground, the position of the lower leg segment in the sagittal plane, which is defined here by the horizontal and vertical position of the knee, x_{knee} and y_{knee}, and the angular orientation of the lower leg segment with respect to vertical, θ_{LL}, are determined at each time-step from the deformation of the foot. The LLTE value is a root-mean-square (RMS) error comparing the trajectory of the modeled lower leg segment to the target lower leg kinematic values of the reference dataset. That is

$$\text{LLTE} \equiv \left[\frac{1}{N}\sum_{n=1}^{N}\left\{\left(\frac{x_{\text{knee},n}^{\text{model}} - x_{\text{knee},n}^{\text{ref}}}{\bar{x}_{\text{knee}}^{\text{ref}}}\right)^2 + \left(\frac{y_{\text{knee},n}^{\text{model}} - y_{\text{knee},n}^{\text{ref}}}{\bar{y}_{\text{knee}}^{\text{ref}}}\right)^2 + \left(\frac{\theta_{\text{LL},n}^{\text{model}} - \theta_{\text{LL},n}^{\text{ref}}}{\bar{\theta}_{\text{LL}}^{\text{ref}}}\right)^2\right\}\right]^{\frac{1}{2}} \tag{1}$$

where the superscripts model and ref refer to values calculated by the constitutive model and from the reference dataset, respectively. The variable N is the total number of time intervals included in the calculation, with subscript n indicating each individual time-step. Each term is normalized by the mean of the reference variable across the portion of the step considered, notated as $\bar{x}_{\text{knee}}^{\text{ref}}$, etc. A thorough justification for the reference normalization factors in Eq. (1) is detailed in previous work [34].

The LLTE framework uses Eq. (1) as a cost function, through which different constitutive models of prosthetic feet can be evaluated by how well they replicate a given desired kinematic dataset under a corresponding kinetic dataset. This process is akin to optimizing the stiffness k of a linear elastic spring with behavior $F = k\delta$ to achieve a desired δ under an applied force F. A prosthetic foot's constitutive model whose LLTE = 0 would perfectly map the reference kinematic data to the reference kinetic data. With LLTE values >0, some deviation—either in kinematics, kinetics, or both—would be expected. The LLTE value also has some relative meaning, in that feet with large LLTE values would be expected to perform worse than feet with lower LLTE values.

The LLTE framework is agnostic to the chosen reference dataset; alternate GRF inputs and kinematic targets could be selected for other objectives such as patient comfort, stability, walking speed, start-stop motions, or walking on nonflat terrain. In this study, Winter's dataset [35] was used as the reference for the LLTE framework. It is from a typical female subject of 56.7 kg with a leg length of 0.83 m. Able-bodied data were chosen as the reference because there is no consensus on what the "ideal" gait should be for a transtibial amputee using a prosthetic foot. Furthermore, the data from Ref. [35] provided a complete kinematic and kinetic reference dataset under known walking conditions (flat ground at self-selected speed of 1.42 m/s, or Froude number (Fr) = 0.25, defined as $\text{Fr} = v^2/gL$ with v the walking speed, g gravity, and L the subject's leg length) that could be replicated in a motion capture lab. The decision to use a symmetric kinematic and kinetic dataset is also based on the assumptions that the load an amputee would apply to the foot would be similar to the load an able-bodied person of the same body mass would apply to the foot, and that symmetric gait is desirable for the user due to the superior esthetics and the reduced risk of long term compensatory injuries [36–39].

This research is motivated by the need to produce low-cost energy storage and return (ESAR) feet for developing countries, driven by our partner, Bhagwan Mahaveer Viklang Sahayata Samiti (BMVSS), in Jaipur, India, the largest distributor of prosthetic limbs in the world. For BMVSS's clients, symmetry is particularly important in order to appear able-bodied and thus avoid stigmas associated with disability. Therefore, there was a user-centered motivation to use physiological gait data as the references in the LLTE framework for this study.

2 Methods

2.1 Experimental Prosthetic Foot Design. An elastic, ESAR foot was designed specifically for this study based on our previous work in which simple conceptual prosthetic feet were optimized to minimize the LLTE value from Eq. (1) [34]. The basic architecture of the foot consists of a pin joint at the ankle with constant rotational stiffness, k_{ank}, and a flexible forefoot with bending stiffness EI, where E is the modulus of elasticity and I is the area moment of inertia (Fig. 1). The ankle stiffness is controlled by U-shaped flexures that can be exchanged to alter the ankle stiffness value. The geometry of the forefoot was selected via the LLTE framework to achieve the predicted optimal forefoot bending stiffness. The remainder of the foot structure was designed to be rigid relative to these flexible components. A full description of the mechanical design of the foot can be found in Ref. [40].

The LLTE-optimal design (corresponding to the minimum LLTE value) for this conceptual foot architecture was previously

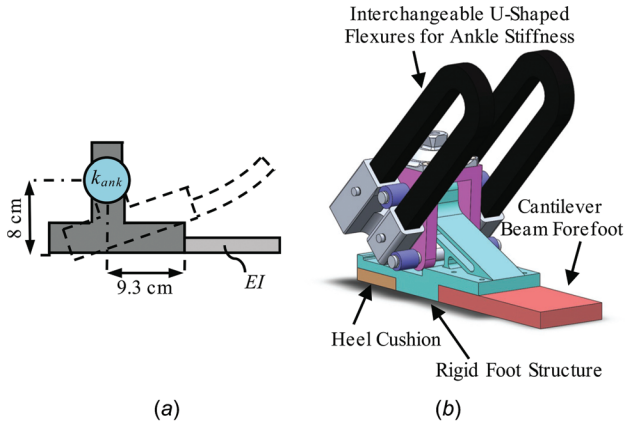

Fig. 1 Schematics of the experimental prosthetic foot. (*a*) The conceptual architecture of the foot optimized with the LLTE framework [34]. The foot consists of a pin joint with constant rotational stiffness at the ankle and a flexible forefoot. The geometry of the foot was selected to replicate the articulation of the biological foot/ankle complex and was not included as a design variable to be optimized. (*b*) Solid model of the experimental foot built to function like the simple foot model in (*a*) [40]. The geometry of the U-shaped flexures dictates the stiffness of the ankle and can be substituted with other flexures to vary the ankle stiffness.

found in Ref. [34] to have stiffnesses $k_{ank} = 3.7$ N·m/deg and $EI = 16.0$ N·m^2. The actual ankle stiffness achieved by our design is 3.6 N·m/deg, which was within the dictated manufacturing tolerances. The forefoot bending stiffness matched the predicted optimal value of 16.0 N·m^2.

Four additional designs with varying ankle stiffnesses were built to explore the sensitivity of the optimized design and investigate how variations in foot stiffness affect walking performance. Ankle stiffness was chosen as the variable to be modified for sensitivity exploration since the LLTE value for this architecture is more sensitive to ankle stiffness than it is to forefoot bending stiffness in the vicinity of the LLTE-optimal design (Fig. 2). Five different ankle stiffnesses were tested in this study while the forefoot bending stiffness was held constant at the predicted optimal value of 16.0 N·m^2 for all conditions. The ankle stiffness values tested were 1.5 N·m/deg, 2.9 N·m/deg, 3.6 N·m/deg, 4.9 N·m/deg, and 24.4 N·m/deg, labeled conditions A–E in order of increasing stiffness, with condition C being our predicted optimal condition.

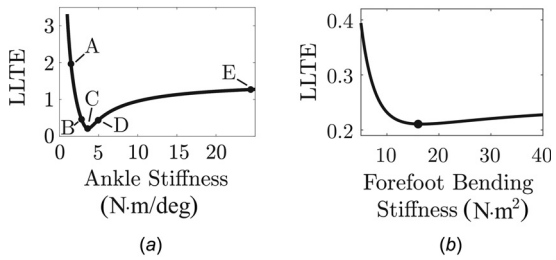

Fig. 2 LLTE values calculated for the foot architecture shown in Fig. 1 for (*a*) ankle stiffnesses ranging from 1 N·m/deg to 25 N·m/deg with the bending stiffness of the forefoot held constant at the LLTE-optimal value, $EI = 16$ N·m/deg, and (*b*) for forefoot bending stiffness ranging from 2 N·m^2 to 40 N·m^2 with the ankle stiffness held constant at the LLTE-optimal value, $k_{ank} = 3.7$ N·m/deg. Since the LLTE value is more sensitive to ankle stiffness than forefoot stiffness, the five experimental feet used in this study had five different ankle stiffnesses, labeled A–E in (*a*), with ankle stiffness C being the predicted optimal stiffness (minimum LLTE value). All of the experimental feet had a constant forefoot beam bending stiffness $EI = 16$ N·m/deg.

The stiffnesses for conditions B and D, as well as conditions A and E were chosen such that their LLTE values would be, respectively, two times and one order of magnitude higher than the LLTE value of condition C, the predicted optimal ankle stiffness. In addition to spanning a wide range of predicted LLTE values, these ankle stiffness values approximately correspond to biological ankle quasi-stiffness values as measured during different phases of gait (1.5–24.4 N·m/deg) [41–43] as well as some commercially available prostheses (3.1–16 N·m/deg) [21,44].

The experimental foot was tested on an Instron material testing machine (Instron, Norwood, MA) with each set of ankle flexures. Every ankle stiffness matched the specified value to within $R^2 = 0.98$, and each demonstrated elastic behavior with minimal hysteresis and viscoelastic behavior [40]. Conditions A–C could safely reach a dorsiflexion angle of 26 deg without the material yielding and before hitting a hard stop. Condition D could reach 25 deg before yielding. These angles are larger than that expected during typical walking (20 deg [45]). Condition E used a hard stop only, rather than a U-shaped spring, to achieve a high enough stiffness, and had a maximum dorsiflexion angle of 6 deg before yielding. For conditions D and E, the maximum deflection would only occur under an ankle moment much larger than those expected during typical walking.

The rigid structure of the foot was machined from acetal resin. Nylon 6/6 was chosen for the U-shaped flexures and the forefoot, as nylon has a high ratio of yield strength (82.7 MPa) to elastic modulus (2.59 GPa), (McMaster-Carr, Inc, Elmhurst, IL) compared to other polymers, which allows the material to undergo large deformations before yielding. The ankle joint was designed such that it could not plantarflex beyond the neutral position to limit the scope of this study to the controlled dorsiflexion portion of stance phase (during which the LLTE value is calculated). The experimental foot was intended to be tested barefoot so that the presence of a shoe would not influence the mechanical behavior. An ethylene-vinyl acetate heel cushion with Shore A Durometer 35–40 was incorporated to minimize shock at heel strike. Rubber soling material intended for athletic shoes was epoxied to the bottom of the foot to provide traction. As tested, the mass of the foot ranged from 930 g to 1330 g, depending on the specific set of U-shaped flexures.

2.2 Data Collection. This research was conducted under the approval of the Committee on the Use of Humans as Experimental Subjects (COUHES) at the Massachusetts Institute of Technology. A single subject with unilateral transtibial amputation was used for this study. This particular subject was selected because her body mass (55.6 kg on average across the multiple testing sessions) and her leg length (0.87 m) were similar to those of the subject in Winter's published gait data (56.7 kg and 0.83 m) [35].

Due to timing constraints, and to avoid fatiguing the subject, data were collected during two visits. In the first visit, conditions D, B, and C were tested (in that order). In the subsequent visit, conditions E, C, A, and C were tested (in that order). Condition C (the LLTE-optimal) was tested on three occasions to ensure repeatability.

At the start of each visit, a qualified prosthetist fit the experimental foot to the subject's usual socket. A new pylon was used in place of the subject's own pylon so that the overall height of the prosthesis was appropriate when the subject wore their own shoe on their sound limb, with no shoe on the prosthetic foot. After the prosthetist performed static and dynamic alignment similar to established clinical practices, the subject was given as much time as needed to acclimate to the foot. Reflective markers were then placed on the subject by a trained technician according to the Helen Hayes marker set [46], with additional markers on the prosthetic foot such that each component of the foot had a minimum of two markers defining its position in the sagittal plane. A digital motion capture system (Motion Analysis Corporation, Santa Rosa, CA) was used to collect kinematic data at 120 Hz. Six force plates

(Advanced Mechanical Technology, Inc., Watertown, MA) embedded in the floor collected kinetic data at 960 Hz. After a static trial, the subject was instructed to walk back and forth along a 10 m walkway at a self-selected comfortable speed. Data from steps were only used if the subject's entire foot landed on a single force plate, and her opposite foot did not contact that same force plate. After five steps were collected on each side, the prosthesis was doffed and the U-shaped flexures were substituted for the next set without removing the foot from the rest of the prosthesis, so as to maintain the same alignment and marker locations for all the conditions. With the new flexures in place, the subject once again donned the prosthesis. The trial procedure was then repeated after a resting and acclimation period. The alignment was unchanged for all the conditions in order to systematically investigate the effect of varying ankle stiffness, as it has been shown that altering the alignment of a prosthetic foot affects the user's walking pattern [25,47].

2.3 Data Analysis

2.3.1 Constitutive Model Validation. Under quasi-static conditions (which occur during stance phase [25]), the output motion of a lower leg prosthesis of known mechanical behavior can be accurately calculated from a set of input GRF and CoP position data. This idea is analogous to a spring governed by $F = k\delta$, where F is the applied force, k is the stiffness, and δ is the resulting deflection. The deterministic mechanical behavior of a lower leg prosthesis does not preclude different users of the same foot exhibiting different gait behaviors; these variations are due to changes in loading and kinematics while the constitutive behavior remains constant (akin to variations in F with changes in δ for a spring with constant k).

To validate our constitutive model, the position of the knee (x_{knee} and y_{knee}) and orientation of the lower leg segment (θ_{LL}) were predicted using measured GRF and CoP data applied to the mechanical model of the experimental prosthetic foot in Fig. 1. These calculations were similar to those performed in the initial design optimization explained in Sec. 1.1, but instead of using published able-bodied data, the kinetic data measured during in vivo testing from each ankle spring configuration were used. The expected position of the lower leg segment was calculated using

$$\begin{aligned}\theta_{\text{LL}} &= \theta_{\text{ank}} + \theta_{ff} \\ &= \frac{M_{\text{ank}}}{k_{\text{ank}}} + \theta_{ff} \\ &= \frac{1}{k_{\text{ank}}}(\text{GRF}_y \cdot x_{cp} + \text{GRF}_x \cdot h) + \theta_{ff}\end{aligned} \tag{2}$$

$$\begin{aligned}x_{\text{knee}} &= x_{\text{ank}} + L_{\text{LL}} \cdot \sin(\theta_{\text{LL}}) \\ &= x_{cp} \cdot (1 - \cos(\theta_{ff})) + L_{\text{LL}} \cdot \sin(\theta_{\text{LL}}), \text{ and}\end{aligned} \tag{3}$$

$$\begin{aligned}y_{\text{knee}} &= y_{\text{ank}} + L_{\text{LL}} \cdot \cos(\theta_{\text{LL}}) \\ &= x_{cp} \cdot \sin(\theta_{ff}) + h \cdot \cos(\theta_{ff}) + L_{\text{LL}} \cdot \cos(\theta_{\text{LL}})\end{aligned} \tag{4}$$

where θ_{ff} is the angle of the foot relative to the ground due to deformation in the forefoot, θ_{ank} is the ankle angle, x_{ank} and y_{ank} are the horizontal and vertical position of the ankle, M_{ank} is the moment about the ankle, and h is the height of the center of the ankle pin joint off the ground when the foot is flat on the ground, which is defined by the geometry of the prototype (Fig. 3). In this case, $h = 0.08$ m. θ_{ff} was calculated iteratively using the Euler–Bernoulli beam bending method, as the component of the GRF transverse to the beam could not be found without knowing this angle, and vice versa. Details of this calculation are published in Ref. [48].

The above calculations rely on the position of the lower leg segment being fully defined by the position of the CoP along the ground, the physical interaction between the ground and the foot, and the no-slip assumption between the ground and the foot. This is not the case for the portion of stance phase immediately following heel strike and preceding toe-off, during which time the foot is in line-contact with the ground. At heel strike, the entire lower leg system rotates about the stationary center of pressure at the heel. At toe-off, the same happens about the toe. During these times, the angle of the prosthesis relative to the ground cannot be determined from the CoP position and GRF data without making additional assumptions about the subject's motion. The experimental feet used in this study were incapable of plantar flexion beyond the neutral position, so there was no motion within the foot until the applied moment (causing dorsiflexion) became greater than zero. Therefore, only the portion of stance for which both (1) the moment about the ankle, M_{ank}, was greater than zero, and (2) the center of pressure was progressing forward, was considered when predicting the output motion of the lower leg (for the constitutive model validation).

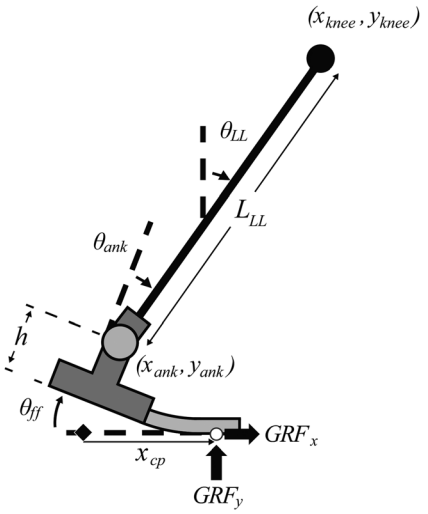

Fig. 3 Graphical definition of variables used in Eqs. (2)–(4) to calculate the position of the lower leg segment under a particular set of GRFs and CoP positions

The variables x_{knee}, y_{knee}, and θ_{LL} were all defined based on the position of a single "knee" point that, under the assumptions of this analysis, lay on an imaginary vertical line drawn through the ankle joint when the foot was flat on the ground and unloaded. It was not expected that the knee joint motion tracking marker used during data collection would lie exactly on this vertical line, as the subject's socket covered her biological knee making anatomical features difficult to locate. To account for this discrepancy, a virtual knee marker was defined in postprocessing to be located at the same distance from the ankle as the physical knee marker, but positioned vertically above the ankle when the foot is on the ground and unloaded. This virtual knee marker was assumed to be part of the same rigid body segment as the physical ankle and knee markers, so the offset angle between the virtual knee marker, the ankle marker, and the physical knee marker was kept constant.

2.3.2 Evaluating the Lower Leg Trajectory Error-Optimized Foot's in vivo Kinematics and Kinetics. The stiffness of the foot model was optimized to most closely connect the kinematic and kinetic data from a reference dataset, in our case Winter's able-body dataset [35]. During this optimization process, six variables were used from able-bodied gait data. The horizontal (fore-aft) and vertical GRFs and CoP position data defined the load on the foot. The horizontal and vertical positions of the knee and the orientation of the lower leg segment were used as our target kinematics. To account for anatomical differences between the test subject and the source of the physiological data, GRFs were scaled by body weight. To reduce potential errors linked to marker placement, all variables describing positions or distances (x_{knee},

Table 1 Subject's average self-selected walking speed for each ankle condition was within one standard deviation of normative average self-selected walking speed [51–53]

Condition	Walking speed (m/s)	Froude number
A	1.31 ± 0.05	0.20 ± 0.02
B	1.28 ± 0.03	0.19 ± 0.01
C	1.37 ± 0.04	0.22 ± 0.01
D	1.20 ± 0.06	0.17 ± 0.02
E	1.35 ± 0.03	0.21 ± 0.01

y_{knee}, and x_{cp}) were scaled by characteristic dimensions. The knee coordinates were scaled by the ratio of the vertical distance from the knee marker to the floor during standing

$$x_{\text{knee}}^{\text{ref}} = x_{\text{knee}}^{W} \frac{L^{\text{meas}}}{L^{W}} \tag{5}$$

where $x_{\text{knee}}^{\text{ref}}$ is the reference value to which the data collected in this study were compared, x_{knee}^{W} is the horizontal position of the knee as published by Winter [35], L^{meas} is the distance from the knee to the ground measured for the subject in this study from the marker set during the static standing trials, and L^{W} is the distance from the knee marker to the ground for the subject in Winter's data. The CoP data were similarly scaled by the ratio of foot lengths. The timing of each variable was normalized over stance phase such that heel strike occurred at 0% and toe-off at 100%. These six variables from able-bodied gait data were then compared using RMS error to the same variables measured during in vivo testing of the prototype feet to evaluate how closely the designed foot could replicate the reference kinematic and kinetic dataset. In addition, these RMS errors were normalized using the individual's physical characteristics, to reduce any biases toward any of the parameters. GRFs were normalized by body weight, CoP was normalized by foot length, the horizontal and vertical knee positions were normalized by L^{meas}, and the lower leg orientation by its angular range of motion.

2.3.3 Assessing the Influence of Foot Stiffness Deviations on Walking Characteristics. One goal of the LLTE framework is to predict the stiffness and geometry of a prosthetic foot design that most closely yields a desired biomechanical response. When using Winter's reference data [35] to design the specific foot model used in this work, the LLTE-optimal ankle stiffness was found to be 3.7 N·m/deg, corresponding to condition C in our study. Any changes from that ankle stiffness should induce some additional deviations in kinematics and/or kinetics of the user's gait mechanics.

Since the LLTE framework targets a reference set of kinematics and kinetics, the effectiveness of each of the tested feet can be measured by computing the normalized RMS (NRMS) errors between the measured and target reference kinematic and kinetic data for each condition, for both the prosthetic and intact limb over the entire stance phase. The deviations from the reference target dataset (in this case, physiological data) were grouped into three scores: one including GRF deviations (vertical and horizontal) (Eq. (6)), one for CoP progression deviation (Eq. (7)), and one for lower leg kinematic deviations (knee position and lower leg orientation in the sagittal plane) (Eq. (8))

$$\Delta_{\text{GRFs}} \equiv \left[\frac{1}{N}\sum_{n=1}^{N}\left(\frac{\text{GRF}_{y,n}^{\text{meas}} - \text{GRF}_{y,n}^{\text{ref}}}{m_{\text{subj}} g}\right)^2\right]^{\frac{1}{2}} + \left[\frac{1}{N}\sum_{n=1}^{N}\left(\frac{\text{GRF}_{x,n}^{\text{meas}} - \text{GRF}_{x,n}^{\text{ref}}}{m_{\text{subj}} g}\right)^2\right]^{\frac{1}{2}} \tag{6}$$

$$\Delta_{\text{CoP}} \equiv \left[\frac{1}{N}\sum_{n=1}^{N}\left(\frac{x_{cp,n}^{\text{meas}} - x_{cp,n}^{\text{ref}}}{l_{\text{foot}}}\right)^2\right]^{\frac{1}{2}} \tag{7}$$

$$\Delta_{\text{kinematics}} \equiv \left[\frac{1}{N}\sum_{n=1}^{N}\left(\frac{x_{\text{knee},n}^{\text{meas}} - x_{\text{knee},n}^{\text{ref}}}{L^{\text{meas}}}\right)^2\right]^{\frac{1}{2}} + \left[\frac{1}{N}\sum_{n=1}^{N}\left(\frac{y_{\text{knee},n}^{\text{meas}} - y_{\text{knee},n}^{\text{ref}}}{L^{meas}}\right)^2\right]^{\frac{1}{2}} + \left[\frac{1}{N}\sum_{n=1}^{N}\left(\frac{\theta_{\text{LL},n}^{\text{meas}} - \theta_{\text{LL},n}^{\text{ref}}}{\theta_{\text{LL,range}}^{\text{ref}}}\right)^2\right]^{\frac{1}{2}} \tag{8}$$

The scores in Eqs. (6)–(8) summarize the level of deviation from a target reference walking pattern exhibited by the individual while walking on level ground at their self-selected speed. The goal of the LLTE design framework is to create a prosthetic foot that enables a user to replicate the target reference walking pattern on both the affected and nonaffected leg. Both legs were considered in our error calculation since compensatory motions and loading are usually exhibited on both sides for unilateral amputees [3,22,31,49,50]. These error scores were then normalized as discussed earlier (Sec. 2.3.2) in order to reduce biases toward any of the parameters. We evaluated differences between conditions using one-way analysis of variances and pairwise comparisons using a Bonferroni adjustment. Statistical significance was set for $p < 0.05$.

3 Results and Discussion

Fifteen steps were collected for stiffness condition C and five steps were collected for stiffness conditions A, B, D, and E, for both the sound and the prosthetic side. The average self-selected walking speeds measured for each ankle are summarized in Table 1. All of these values were within one standard deviation of normative average self-selected walking speed (Fr = 0.23 ± 0.07 [51–53]), but lower than the reference data of 1.42 m/s (Fr = 0.25).

3.1 Accuracy of the Constitutive Model. Using the foot constitutive model, the x_{knee}, y_{knee}, and θ_{LL} values were predicted from the measured GRF and CoP values for each individual prosthetic step, for a total of 35 steps, and compared to the corresponding measured kinematic values (Fig. 4). Across all of the collected data points, the average absolute differences between the predicted and measured values for each of these variables were 1.0 cm for x_{knee}, 0.3 cm for y_{knee}, and 1.5 deg for θ_{LL}.

The ankle angle–moment curves as measured during gait testing were compared to the mechanical behavior of the experimental foot ankle joint as measured on an Instron machine (Fig. 5). During the controlled dorsiflexion phase of stance, the in situ ankle angle–moment curves fit the Instron measured experimental foot behavior with R^2 values of 0.68, 0.94, 0.82, 0.92, and −0.19 for conditions A–E, respectively. The results demonstrate that the analytical model of a pin joint with the specified constant rotational stiffness adequately represented the ankle of the experimental foot for conditions A–D. For condition A, Fig. 5 shows an increase in stiffness at 26 deg, corresponding to the ankle hitting the hard stop; the R^2 value reported only applies to the linear elastic region of the curve. It has a lower than expected value due to the smaller ankle moments recorded compared to the other feet, which made it sensitive to the static friction and spring preload. Accounting for the resulting 3.5 N·m of friction and preload that

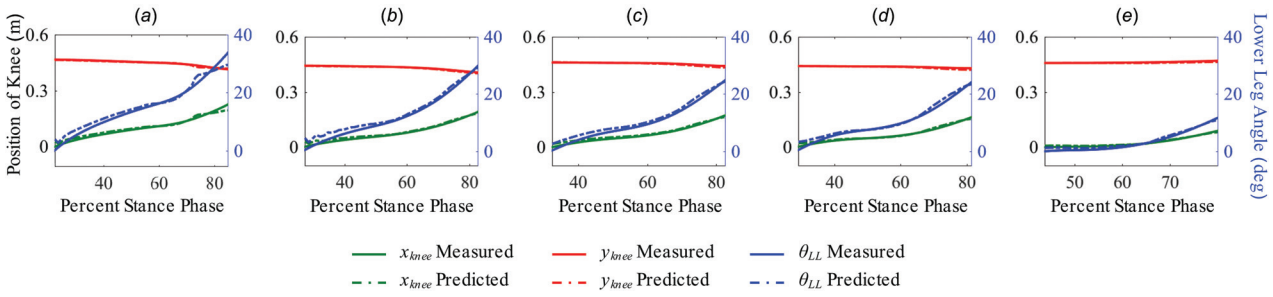

Fig. 4 Lower leg trajectory, defined by x_{knee}, y_{knee}, and θ_{LL}, predicted by the constitutive model using GRF_x, GRF_y, and x_{cp} values measured from the test subject as inputs, compared to the corresponding measured kinematic data. A single representative step is shown for each of the five ankle stiffness conditions. The *x*-axis spans the range of times covered by the model, beginning when the ankle dorsiflexion angle becomes greater than zero, and ending when the center of pressure ceases to progress forward.

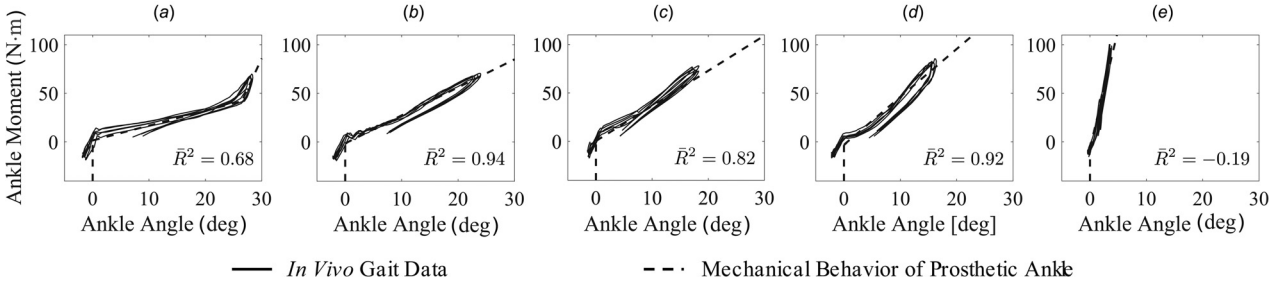

Fig. 5 Ankle moment versus ankle angle measured during in vivo testing for each of the five ankle stiffness conditions. Each solid black line represents one captured prosthetic step; the dashed lines show the ankle stiffnesses measured on an Instron machine. Note in condition A the ankle hit the hard stop at 26 deg, at which point the stiffness increased beyond the expected stiffness.

offsets the measured data, the R^2 value for condition A increases to 0.89, which aligns with the Instron and in vivo measured stiffnesses of 1.54 ± 0.02 N·m/deg and 1.46 ± 0.04 N·m/deg, respectively. Similarly, by taking into account the static friction and spring preload values for conditions B–E, the corresponding fitted curves R^2 values increase to 0.98, 0.91, 0.96, and 0.20 for condition B–E, respectively. For condition E, the negative R^2 value (or low positive R^2 when accounting for friction and preload) indicates that the ankle behavior as measured on the Instron machine does not describe its mechanical behavior as measured during in vivo testing. This is due to the small range of motion of the ankle, which causes the fit of the in vivo and Instron data to be sensitive to the neutral, unloaded position of the ankle, which is calculated using swing phase data. If the neutral ankle angle is decreased by 1 deg from the angle found during swing phase, the R^2 value for condition E increases to 0.88.

As evidenced by both the measured x_{knee} and θ_{LL} values in Fig. 4 and the ankle angle–moment curves in Fig. 5, the large variation in ankle stiffness of the prototype feet affected the subject's gait mechanics. The constitutive model accurately predicted lower leg kinematics for each ankle stiffness condition. These results indicate that the assumptions of the model—no-slip between the foot and the ground, quasi-static deformation of the foot during stance, and rigid prosthetic socket and pylon—are reasonably accurate during the controlled dorsiflexion portion of stance phase. The results of Fig. 5 also validate the elastic behavior of the foot prototype. The ankle–moment curves show little hysteresis and match the stiffnesses measured quasi-statically on the Instron machine. Figures 4 and 5 quantitatively demonstrate the LLTE framework constitutive model's ability to compute the biomechanical response of a patient given a foot's mechanical design, and an applied kinetic dataset, under a wide range of ankle stiffness conditions.

As previously discussed, the model can only be used to calculate the lower leg trajectory during foot-flat; prior to this, the foot is pivoting about a line contact at the heel, so the orientation of the prosthesis is indeterminate. Once the moment about the ankle becomes positive, the model can be used to calculate the lower leg trajectory until the heel and most of the forefoot lift off the ground, at which point the foot is pivoting about the tip of the toe. This time was identified in the gait data as the instant the CoP ceased to progress forward. Consequently, the portion of stance for which the lower leg trajectory could be predicted varied for each foot: 60% for the able-body condition and 59%, 53%, 50%, 49%, and 42% for conditions A–E, respectively. This does not mean that the subject spent less time in stance on the foot with ankle stiffness condition E than with condition A, but rather that, of the time she was in stance on the prosthetic side for condition E, she spent less of that time with her foot flat on the ground in controlled dorsiflexion and more time pivoting about the heel or toe.

3.2 Lower Leg Trajectory Error-Optimized Foot's Replication of Target Kinematics and Kinetics. Lower leg trajectory error-optimized foot C is the only variant in this study for which the LLTE framework has full predictive capability. This is because foot C represents a minimum of the LLTE function, meaning we would expect it to yield close-to able-bodied kinematics when subjected to able-bodied kinetics. The other feet tested in this study have LLTE values that were intentionally varied away from the optimum; this means we would expect them to behave worse than foot C, but we cannot quantitatively predict what their biomechanical response would be. As such, in this subsection, we compare the kinematic and kinetic responses of foot C to the physiological targets used in the LLTE framework, exploring how well the framework was able to generate a foot design that yielded the desired response.

Measured kinematic and kinetic data (x_{knee}, y_{knee}, θ_{LL}, GRF_y, GRF_x, and x_{cp}) from the LLTE-optimal condition C for both the

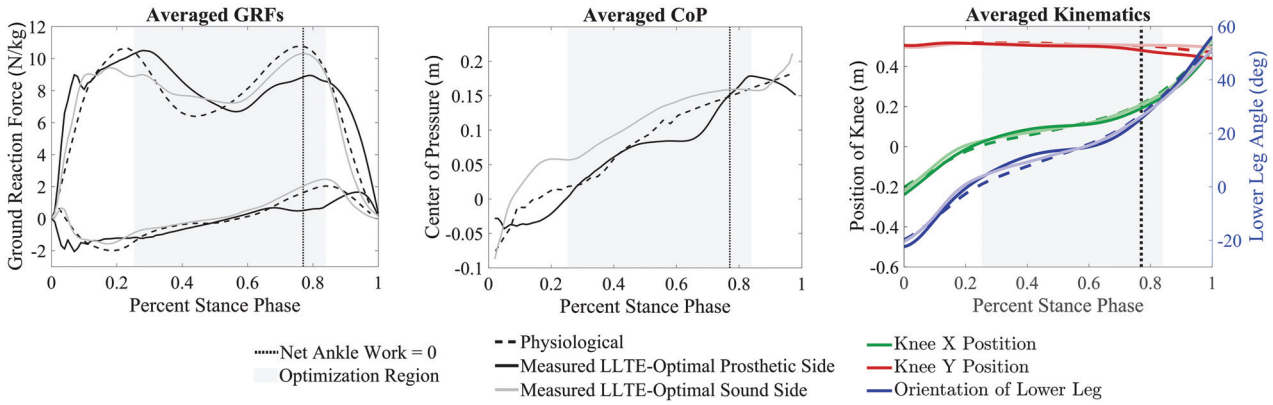

Fig. 6 Average kinetic and kinematic variables over the entire stance phase. Data were measured during in vivo testing for the LLTE-optimal ankle stiffness $k_{ank} = 3.7$ N·m/deg, condition C, for both the prosthetic and sound sides compared to the corresponding reference physiological data used in the LLTE framework to optimize the foot. The vertical dotted line marks the moment in stance when the net work done by the biological ankle joint becomes positive. The gray shaded region represents the stance phase window during which the LLTE value is calculated.

Table 2 Able-bodied gait data compared using a root-mean-square error to the same variables measured during in vivo testing of condition C, showing that the designed LLTE-optimal foot replicated the reference kinematic and kinetic datasets

	RMS values	
Gait parameter	Sound side	Prosthetic side
GRF_x (N)	17 ± 2	40 ± 2
GRF_y (N)	46 ± 7	91 ± 6
CoP (m)	0.027 ± 0.005	0.024 ± 0.007
x_{knee} (m)	0.014 ± 0.002	0.020 ± 0.004
y_{knee} (m)	0.008 ± 0.002	0.015 ± 0.003
θ_{LL} (deg)	1.8 ± 0.3	2.2 ± 0.5

Table 3 Able-bodied gait data compared using a normalized root-mean-square error to the same variables measured during in vivo testing of condition C, showing that the designed LLTE-optimal foot replicated the reference kinematic dataset within 4% and the kinetic dataset within 16%

	Normalized RMS values	
Gait parameter	Sound side	Prosthetic side
GRF_x	0.03 ± 0.01	0.07 ± 0.01
GRF_y	0.08 ± 0.01	0.16 ± 0.01
CoP	0.10 ± 0.02	0.09 ± 0.03
x_{knee}	0.03 ± 0.01	0.04 ± 0.01
y_{knee}	0.02 ± 0.01	0.03 ± 0.01
θ_{LL}	0.03 ± 0.01	0.03 ± 0.01

sound and prosthetic sides are shown in Fig. 6 compared to Winter's reference physiological data used in the LLTE framework. From these data, RMS errors for each of the measured physical quantities for both the sound and prosthetic sides are summarized in Table 2. To reduce any biases toward any of the parameters, the GRFs were normalized by body weight, the CoP was normalized by foot length, and the knee position was normalized by the height of the knee during quiet standing (Table 3).

Since the passive experimental feet in this study could not generate power, the prosthetic side in vivo data diverge from the physiological data during late stance when the network from the biological ankle over the course of the step becomes positive, indicated by the vertical dotted lines in Fig. 6. This is most noticeable for the horizontal and vertical GRFs and knee vertical position data. Prior to this point in stance, the negative external work done by a physiological ankle exactly balances the positive external work, so it is theoretically possible for a perfectly efficient ESAR foot to exactly replicate physiological kinetic and kinematic data up until this point. When the prosthetic side is not able to replicate physiological values, the corresponding sound side data also diverge, as seen in the reduced sound side vertical GRFs in early stance (Fig. 6).

Despite these differences, the in vivo kinematic variables, x_{knee}, y_{knee}, and θ_{LL}, matched the physiological target data within 4% over stance phase (Table 3). The kinetic variables, GRF_x, GRF_y, and CoP, were also close to the target data, with a maximum error of 16%. Thus, the LLTE-optimized foot design was able to accurately replicate the target physiological gait data. This result aligns with the motivation for this research: to create passive, low-cost ESAR feet that can restore able-bodied walking motion to help amputees in developing countries avoid social stigmas [40].

3.3 Effect of Lower Leg Trajectory Error Values on User's Walking Pattern. NRMS errors that measure how variations in foot stiffness affect walking behavior are shown in Fig. 7. These values were calculated from the measured kinematic and kinetic data for both the sound and prosthetic sides for each stiffness condition A–E according to Eqs. (6)–(8). Figure 7 represents the level of deviation from the reference dataset in terms of errors in GRFs, CoP progression, and lower leg kinematics.

The NRMS error from the measured ground reaction force data (Fig. 7(*a*)) shows that condition E caused the most amount of deviation from the reference data and condition B resulted in the least amount of deviation. The results show a trend in which deviation increases as the ankle stiffness value diverges from condition B. Conditions A–D are statistically different from condition E, with respective p-values of $p_{AE} < 0.001$, $p_{BE} < 0.001$, $p_{CE} < 0.001$, $p_{DE} = 0.011$. In addition, statistical differences occurred between conditions B and D, with $p_{BD} = 0.004$, and conditions C and D, with $p_{CD} = 0.016$.

The NRMS error from the measured CoP progression (Fig. 7(*b*)) shows that condition E caused significantly more deviation from the reference data than the other conditions. In addition, conditions B and D resulted in the least amount of deviation, significantly lower than condition C and E, but not condition A, with $p_{BA} = 0.378$ and $p_{DA} = 0.272$. There was not any correlation between ankle stiffness and CoP deviation from the reference target data.

The NRMS error from the measured kinematic data (Fig. 7(*c*)) shows that conditions A and E caused statistically more deviation

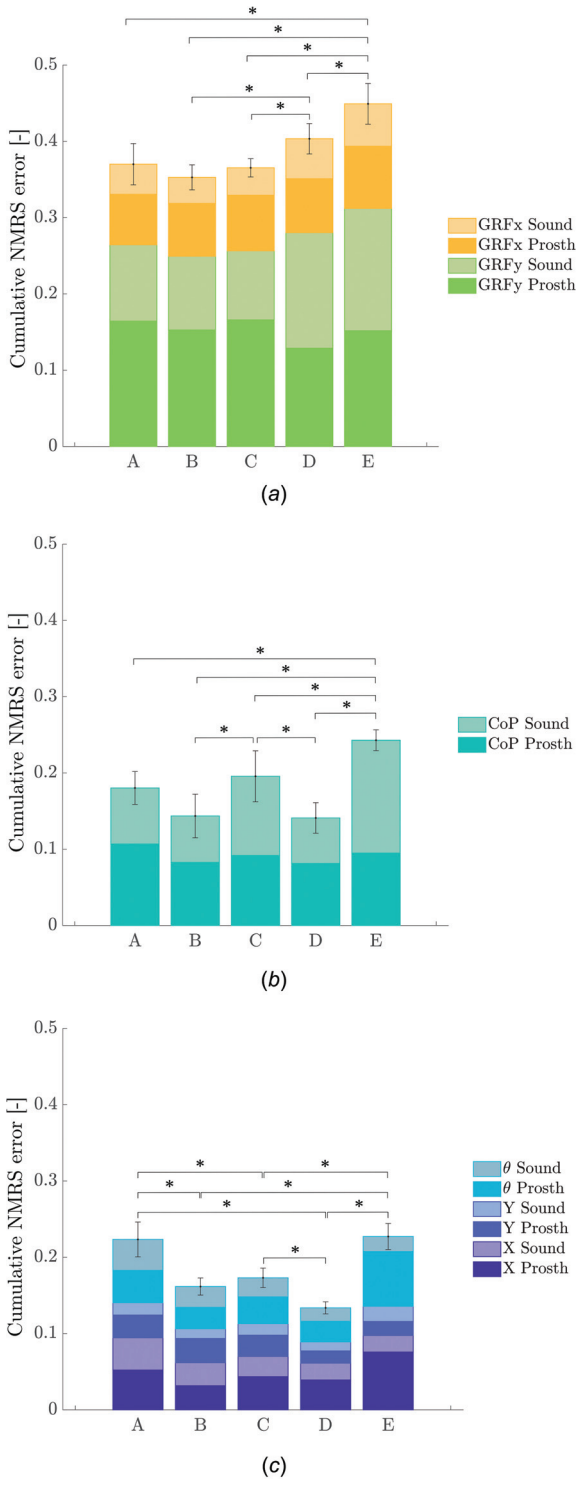

Fig. 7 Cumulative NRMS error between physiological data and: (*a*) GRF data, (*b*) CoP data, and (*c*) kinematic data across all five ankle stiffness conditions, for both the prosthetic and sound sides, and for all collected steps. The error bars for each condition indicate the variance between each step for a given condition, and the conditions marked with * have a pairwise *p*-value $p < 0.05$. Condition A is the most compliant ankle, E is the stiffest, and C is the LLTE-optimal.

from the reference data compared to conditions B, C, and D with p-values $p < 0.001$ for each pairwise comparison. Condition D resulted in the least amount of deviation, significantly lower than conditions A, E, and C with $p_{CD} = 0.001$, and marginally

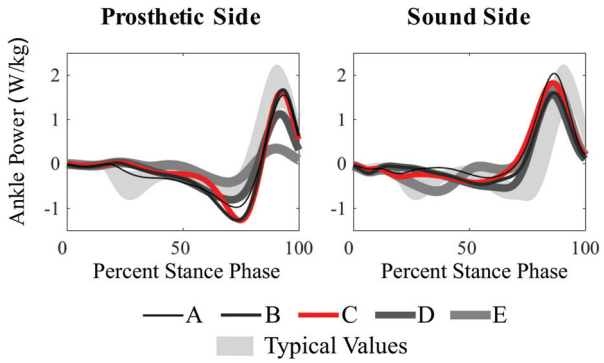

Fig. 8 Average ankle joint power over the entire stance phase for both the prosthetic and sound legs, for all stiffness conditions. The sound leg exhibited similar joint power for all conditions. On the prosthetic side, conditions A–C stored and returned more energy, and enabled an increased ankle push-off power compared to conditions D and E.

significantly lower than condition B with $p_{BD} = 0.054$. The level of deviation was lower for kinematic variables (Tables 2 and 3), with an average NRMS error of 3.5%, compared with kinetic variables, with an average NRMS error of 10.6%.

Ankle joint power for each condition and each leg compared with typical normative data is shown in Fig. 8. The sound leg exhibited similar push-off power and timing for all conditions. On the prosthetic side, the lower stiffness conditions A–C enabled increased stored and returned energy and peak push-off power compared with the high stiffness conditions D and E. This aligns with previous findings suggesting that lower stiffness prosthetic feet induced increased ankle push-off power and energy storage [8,54,55]. In addition, this result reinforces the findings from Fey et al. [22], suggesting that there is a limit at which decreasing the ankle stiffness will not increase energy storage and push-off power; the lower stiffness conditions A and B provided similar peak push-off power and timing compared with condition C, the predicted optimal stiffness condition.

The data from a single subject, as was used in this study, are insufficient to draw definitive conclusions about how persons with unilateral transtibial amputations will generally respond to five feet with varying LLTE values. However, since the ultimate goal of optimizing feet with the LLTE framework is to deterministically design prosthetic feet that offer some benefits to the user, the differences in gait mechanics observed in this single-subject study are meaningful. The kinematic data error plot (Fig. 7(*c*)) indicates that stiffness conditions far from the LLTE-optimal condition deviated the most from the target reference kinematic data. This aligns with the fact that conditions B, C, and D had lower LLTE values (respectively, 0.382, 0.222, and 0.452) compared with conditions A and E (respectively, 1.96 and 1.14), as seen in Fig. 2. This also matches the subject's feedback regarding each of the tested feet, in which conditions B, C, and D were stated as the preferred feet over conditions A and E. The subject clearly stated her discomfort and dislike toward conditions A and E, but could not say which of conditions B, C, or D she liked the most. This indicates that the LLTE framework seems to discriminate prosthetic feet with high LLTE values, but is less sensitive to prosthetic foot designs around the LLTE-optimal. From these findings, it is too soon to define the exact sensitivity of LLTE values and their impact on walking biomechanics; the presented results show meaningful trends. Further experimental work with additional subjects and a variety of prosthetic foot architectures is required to fully understand and assess the sensitivity of LLTE predictions.

The trend apparent in the kinematic data—that prosthetic feet with lower LLTE values induced better mechanics—was not clearly displayed in the kinetic data. However, the amount of deviation was three times lower on average for kinematic

Table 4 LLTE-optimal ankle stiffnesses, for example, individuals with increasing body mass, using the specific foot architecture described in this study [40]

User mass	LLTE-optimal ankle stiffness
40 kg	2.55 N·m/deg
50 kg	3.21 N·m/deg
60 kg	3.93 N·m/deg
70 kg	4.65 N·m/deg
80 kg	5.42 N·m/deg
90 kg	6.25 N·m/deg

variables compared with kinetic variables (as seen in Figs. 6 and 7, and Table 3), suggesting that the particular subject in this study walked in such a way as to maintain close-to physiological motion regardless of the foot she was given. This suggests that using physiological kinematic data as target reference data in designing a prosthetic foot with the LLTE framework would be appropriate. This is not to say that able-bodied gait data are the only reasonable choice for model inputs; physiological data were a logical choice for this study because they provided a benchmark for comparison to our theory, and because able-bodied appearance is desired by our target users in India. The LLTE framework could just as easily be utilized with another gait objective, such as obtaining a specific asymmetric gait, which, according to some simulation studies, may decrease the metabolic cost of walking [56].

The fact that feet B and D behaved similarly to the LLTE-optimized foot C could actually be favorable in the context of commercial prosthetic foot design. This result indicates that feet with LLTE values near the predicted optimal could perform satisfactorily for a patient. This could also facilitate the creation of a prosthetic foot product line, similar to how other feet are made, with discrete sizes and stiffnesses (Table 4). Each foot model could serve patients within a variation of body sizes and weights. This provision model is particularly well suited to our target market in India, as producing fewer variants will help reduce production costs. Feet designed with the LLTE framework may also enable straightforward prescription practices well suited to developing world limb fitment camps, where a technician could use a simple look-up table for a patient's height and weight to determine the correct foot model.

Furthermore, stating that it is appropriate to use physiological data as model inputs and target outputs in designing a prosthetic foot does not imply that the predicted model outputs (in this case, x_{knee}, y_{knee}, and θ_{LL}), which are calculated from the assumed physiological inputs (in this case, GRF_x, GRF_y, and x_{CP}), will always be representative of the actual data measured when a human subject uses the prosthetic foot. If the predicted output kinematics differ significantly from the reference data (that is, the prosthetic foot has a high LLTE value), it is expected that the human user will alter any and/or all aspects of their gait mechanics in an unpredictable manner to make walking with that foot as comfortable as possible, such as varying the loading of the foot or the time spent during foot flat. With such a foot, the specific predicted output motion from the LLTE framework may be meaningless; for example, a low-stiffness ankle that is predicted to have unreasonably large lower leg angles when subjected to physiological GRFs. However, predicting a high LLTE value for a foot is still meaningful, as it indicates that it is not possible for someone to walk on that foot with kinematics and kinetics close to the reference dataset. A foot with a minimized LLTE value, ideally close to 0, is the only prediction with physical meaning, with kinematics and kinetics anticipated to be near the reference data, which was indeed the case for foot C.

While this paper focused on experimentally demonstrating the theory behind the LLTE framework, this pilot study was limited to a single reference walking activity and dataset, as well as a simple proof-of-concept prototype without plantarflexion or inversion/eversion. Future work will include a larger study with multiple subjects who will each test prosthetic feet with stiffnesses and geometries comparable to existing commercially available devices optimized for their given body size, mass, and desired activities, to confirm that prosthetic feet designed with lower LLTE values offer benefits to users. We do not claim that feet with low LLTE values will be superior to existing commercial feet; only proof-of-concept prototypes were tested in this study, and users may value attributes not captured by the LLTE framework (such as weight and standing stability).

4 Conclusions

A single subject with unilateral transtibial amputation tested an experimental foot consisting of a pin joint at the ankle with adjustable stiffness and a flexible forefoot. LLTE-optimal stiffness values were found through the LLTE design framework ($k_{\text{ank}} = 3.7$ N·m/deg and $EI = 17$ N·m^2) using physiological kinematic and kinetic data target values. In addition, the subject tested four varying ankle stiffness conditions above and below the LLTE-optimal value, ranging from 1.5 N·m/deg to 24.4 N·m/deg.

A constitutive model of the foot was built using its stiffness and geometry characteristics and validated using in vivo data. When the measured GRF and CoP data for all stiffness conditions were used as inputs for this constitutive model, the position of the knee joint was predicted within an average error of 1.0 cm in the horizontal direction and 0.3 cm in the vertical direction. The angular orientation of the lower leg segment was predicted within an average error of 1.5 deg. These results demonstrate that the constitutive model behind the LLTE framework accurately predicted the lower leg trajectory under a known set of GRF and CoP data. The foot model used herein assumed an elastic structure (which experimentally exhibited minimal hysteresis). Feet with viscous and/or viscoelastic behavior could also be used in the LLTE framework, provided a viscous term (with forces proportional to deformation rate) were incorporated into the constitutive model.

The LLTE-optimal foot, condition C, enabled the user to replicate the target reference dataset in trend and magnitude within 16% NRMS error. More specifically, the measured kinematic variables—horizontal and vertical positions of the knee, and angular orientation of the lower leg segment—matched the physiological target within 4%. This result demonstrates that a prosthetic foot model optimized using the LLTE framework can replicate a desired biomechanical response.

For the particular subject used in this study, it was observed that the feet with highest LLTE values (A and E) resulted in the greatest deviations in kinematics, while the feet near the minimum (B, C, and D) better replicated the physiological reference data. This suggests that prosthetic feet designed with lower LLTE values could offer benefits to users. In addition, the level of deviation from the physiological reference data was three times lower on average for kinematic variables compared with kinetic variables across all stiffness conditions, indicating that the individual walked in such a way as to maintain close-to able-bodied motion regardless of the foot she was given. This suggests that using physiological kinematic data as target reference data in designing a prosthetic foot with the LLTE framework could be appropriate.

The intent of this study was to experimentally demonstrate a predictive theory that quantitatively connects the mechanical design of a prosthetic foot to its biomechanical performance, is agnostic to specific foot designs, can accept any reference kinematic and kinetic datasets, and may be used as a tool to design, optimize, and customize feet for individual patients. Having such a design tool that provides insights into prosthetic foot design, similar to the Pareto principle, would be most relevant in the context of offering affordable ESAR prosthetic feet to developing countries. The design of these feet could account for a patient's body weight and size, and could be prescribed with a straightforward process like a look-up table.

Acknowledgment

This research was funded by the Tata Center for Technology and Design at MIT. The authors would like to thank Rebecca Stine for her help in collecting and processing the data presented in this work. We would also like to thank Dr. Pooja Mukul, Dr. M. K. Mathur, and D. R. Mehta from Bhagwan Mahaveer Viklang Sahayata Samiti, the Jaipur Foot organization, for their partnership on this research program to design high-performance, low-cost, passive prosthetic feet.

References

[1] Adamczyk, P. G., Arbor, A., Arbor, A., and Hahn, M. E., 2014, "Novel Method to Evaluate Angular Stiffness of Prosthetic Feet From Linear Compression Tests," ASME J. Biomech. Eng., **135**(10), p. 104502.
[2] Zelik, K. E., Collins, S. H., Adamczyk, P. G., Segal, A. D., Klute, G. K., Morgenroth, D. C., Hahn, M. E., Orendurff, M. S., Czerniecki, J. M., and Kuo, A. D., 2011, "Systematic Variation of Prosthetic Foot Spring Affects Center-of-Mass Mechanics and Metabolic Cost During Walking," IEEE Trans. Neural Syst. Rehabil. Eng., **19**(4), pp. 411–419.
[3] Klodd, E., Hansen, A., Fatone, S., and Edwards, M., 2010, "Effects of Prosthetic Foot Forefoot Flexibility on Gait of Unilateral Transtibial Prosthesis Users," J. Rehabil. Res. Dev., **47**(9), pp. 899–910.
[4] Klodd, E., Hansen, A., Fatone, S., and Edwards, M., 2010, "Effects of Prosthetic Foot Forefoot Flexibility on Oxygen Cost and Subjective Preference Rankings of Unilateral Transtibial Prosthesis Users," J. Rehabil. Res. Dev., **47**(6), pp. 543–552.
[5] Postema, K., Hermens, H. J., De Vries, J., Koopman, H. F. J. M., and Eisma, W. H., 1997, "Energy Storage and Release of Prosthetic Feet—Part 1: Biomechanical Analysis Related to User Benefits," Prosthetics Orthotics International, **21**(1), pp. 17–27.
[6] Major, M. J., Twiste, M., Kenney, L. P. J., and Howard, D., 2014, "The Effects of Prosthetic Ankle Stiffness on Ankle and Knee Kinematics, Prosthetic Limb Loading, and Net Metabolic Cost of Trans-Tibial Amputee Gait," Clin. Biomech., **29**(1), pp. 98–104.
[7] Fey, N. P., Klute, G. K., and Neptune, R. R., 2012, "Optimization of Prosthetic Foot Stiffness to Reduce Metabolic Cost and Intact Knee Loading During Below-Knee Amputee Walking: A Theoretical Study," ASME J. Biomech. Eng., **134**(11), p. 111005.
[8] Fey, N. P., Klute, G. K., and Neptune, R. R., 2013, "Altering Prosthetic Foot Stiffness Influences Foot and Muscle Function During Below-Knee Amputee Walking: A Modeling and Simulation Analysis," J. Biomech., **46**(4), pp. 637–644.
[9] Hofstad, C., Linde, H., Limbeek, J., and Postema, K., 2004, "Prescription of Prosthetic Ankle-Foot Mechanisms After Lower Limb Amputation," Cochrane Database Syst. Rev., Issue 1.
[10] Linde, H. V. D., Hofstad, C. J., Geurts, A. C. H., Postema, K., Geertzen, J. H. B., and Limbeek, J. V., 2004, "A Systematic Literature Review of the Effect of Different Prosthetic Components on Human Functioning With a Lower Limb Prosthesis," J. Rehabil. Res. Dev., **41**(4), pp. 555–570.
[11] Major, M. J., Twiste, M., Kenney, L. P. J., and Howard, D., 2011, "Amputee Independent Prosthesis Properties-A New Model for Description and Measurement," J. Biomech., **44**(14), pp. 2572–2575.
[12] Zhao, S. R., Haberman, A., Li, Q., and Bryant, J. T., 2017, "Method for Predicting Deformation Characteristics of Prosthetic Feet," J. Prosthetics Orthotics, **29**(1), pp. 7–18.
[13] Major, M. J., 2010, "The Influence of the Mechanical Properties of Trans-Tibial Prostheses on Amputee Performance," Ph.D. thesis, University of Salford, Salford, UK.
[14] Major, M. J., Kenney, L. P. J., Twiste, M., and Howard, D., 2012, "Stance Phase Mechanical Characterization of Transtibial Prostheses Distal to the Socket: A Review," J. Rehabil. Res. Dev., **49**(6), p. 815.
[15] Geil, M. D., 2001, "Energy Loss and Stiffness Properties of Dynamic Elastic Response Prosthetic Feet," J. Prosthetics Orthotics, **13**(3), pp. 70–73.
[16] Miller, L. A., and Childress, D. S., 1997, "Analysis of a Vertical Compliance Prosthetic Foot," J. Rehabil. Res. Dev., **34**(1), pp. 52–57.
[17] Water, G. J., De Vries, J., and Mulder, M. A., 1998, "Comparison of the Lightweight Camp Normal Activity Foot With Other Prosthetic Feet in Trans-Tibial Amputees: A Pilot Study," Prosthetics Orthotics Int., **22**(2), pp. 107–114.
[18] Geil, M. D., 2002, "An Iterative Method for Viscoelastic Modeling of Prosthetic Feet," J. Biomech., **35**(10), pp. 1405–1410.
[19] Skinner, H. B., Abrahamson, M. A., Hung, R. K., Wilson, L. A., and Effeney, D. J., 1985, "Static Load Response of the Heels of SACH Feet," Orthopedics, **8**(2), pp. 225–228.
[20] Klute, G. K., and Berge, J. S., 2004, "Modelling the Effect of Prosthetic Feet and Shoes on the Heel-Ground Contact Force in Amputee Gait," Proc. Inst. Mech. Eng., Part H, **218**(3), pp. 173–182.
[21] Lehmann, J. F., Price, R., Boswell-Bessette, S., Dralle, A., Questad, K., and DeLateur, B. J., 1993, "Comprehensive Analysis of Energy Storing Prosthetic Feet: Flex Foot and Seattle Foot Versus Standard SACH Foot," Arch. Phys. Med. Rehabil., **74**(11), pp. 1225–1231.
[22] Fey, N. P., Klute, G. K., and Neptune, R. R., 2011, "The Influence of Energy Storage and Return Foot Stiffness on Walking Mechanics and Muscle Activity in Below-Knee Amputees," Clin. Biomech., **26**(10), pp. 1025–1032.
[23] Lee, H., Rouse, E. J., and Krebs, H. I., 2016, "Summary of Human Ankle Mechanical Impedance During Walking," IEEE J. Trans. Eng. Health Med., **4**, pp. 1–7.
[24] Shepherd, M. K., and Rouse, E. J., 2017, "The VSPA Foot: A Quasi-Passive Ankle-Foot Prosthesis With Continuously Variable Stiffness," IEEE Trans. Neural Syst. Rehabil. Eng., **25**(12), pp. 2375–2386.
[25] Hansen, A. H., Childress, D. S., and Knox, E. H., 2000, "Prosthetic Foot Roll-Over Shapes With Implications for Alignment of Trans-Tibial Prostheses," Prosthetics Orthotics Int., **24**(3), pp. 205–215.
[26] Knox, E. H., and Childress, D. S., 1996, "The Role of Prosthetic Feet in Walking," Ph.D. thesis, Chicago Ill: Northwestern University, Evanston, IL.
[27] Sam, M., 2000, "Mechanical Characterization of Prosthetic Feet Using a Prosthetic Foot Loading Apparatus," Eng. Med., **22**(3), pp. 1968–1971.
[28] Sam, M., Hansen, A. H., Childress, D. S., and Hansen, A., 2004, "Characterisation of Prosthetic Feet Used in Low-Income Countries," Prosthetics Orthotics Int., **28**(2), pp. 132–140.
[29] Curtze, C., Hof, A. L., van Keeken, H. G., Halbertsma, J. P. K., Postema, K., and Otten, B., 2009, "Comparative Roll-Over Analysis of Prosthetic Feet," J. Biomech., **42**(11), pp. 1746–1753.
[30] Adamczyk, P. G., Collins, S. H., and Kuo, A. D., 2006, "The Advantages of a Rolling Foot in Human Walking," J. Exp. Biol., **209**(20), pp. 3953–3963.
[31] Adamczyk, P. G., and Kuo, A. D., 2013, "Mechanical and Energetic Consequences of Rolling Foot Shape in Human Walking," J. Exp. Biol., **216**(14), pp. 2722–2731.
[32] Srinivasan, S., Raptis, I. A., and Westervelt, E. R., 2008, "Low-Dimensional Sagittal Plane Model of Normal Human Walking," ASME J. Biomech. Eng., **130**(5), p. 051017.
[33] Olesnavage, K. M., and Winter, A. G., 2015, "Design and Qualitative Testing of a Prosthetic Foot With Rotational Ankle and Metatarsals Joints to Mimic Physiological Roll-Over Shape," ASME Paper No. DETC2015-46518.
[34] Olesnavage, K. M., and Winter, A. G., 2018, "A Novel Framework for Quantitatively Connecting the Mechanical Design of Passive Prosthetic Feet to Lower Leg Trajectory," IEEE Trans. Neural Syst. Rehabil. Eng., **26**(8), pp. 1544–1555.
[35] Winter, D. A., 2009, "Signal Processing," *Biomechanics and Motor Control of Human Movement*, 4th ed., Wiley, Hoboken, NJ.
[36] Gailey, R., Allen, K., Castles, J., Kucharik, J., and Roeder, M., 2008, "Review of Secondary Physical Conditions Associated With Lower-Limb Amputation and Long-Term Prosthesis Use," J. Rehabil. Res. Dev., **45**(1), pp. 15–29.
[37] Norvell, D. C., Czerniecki, J. M., Reiber, G. E., Maynard, C., Pecoraro, J. A., and Weiss, N. S., 2005, "The Prevalence of Knee Pain and Symptomatic Knee Osteoarthritis Among Veteran Traumatic Amputees and Nonamputees," Arch. Phys. Med. Rehabil., **86**(3), pp. 487–493.
[38] Struyf, P. A., van Heugten, C. M., Hitters, M. W., and Smeets, R. J., 2009, "The Prevalence of Osteoarthritis of the Intact Hip and Knee Among Traumatic Leg Amputees," Arch. Phys. Med. Rehabil., **90**(3), pp. 440–446.
[39] Morgan, S. J., Mcdonald, C. L., Halsne, E. G., Cheever, S. M., Salem, R., Kramer, P. A., and Hafner, B. J., 2018, "Laboratory- and Community-Based Health Outcomes in People With Transtibial Amputation Using Crossover and Energy- Storing Prosthetic Feet: A Randomized Crossover Trial," PLoS One, **13**(2), p. e0189652.
[40] Prost, V., Olesnavage, K. M., Johnson, W. B., Major, M. J., and Winter, V. A. G., 2018, "Design and Testing of a Prosthetic Foot With Interchangeable Custom Springs for Evaluating Lower Leg Trajectory Error, an Optimization Metric for Prosthetic Feet," ASME J. Mechanisms Robotics, **10**(2), p. 021010.
[41] Rouse, E. J., Hargrove, L. J., Perreault, E. J., and Kuiken, T. A., 2014, "Estimation of Human Ankle Impedance During the Stance Phase of Walking," IEEE Trans. Neural Syst. Rehabil. Eng., **22**(4), pp. 870–878.
[42] Shamaei, K., Sawicki, G. S., and Dollar, A. M., 2013, "Estimation of Quasi-Stiffness of the Human Hip in the Stance Phase of Walking," PLoS One, **8**(12), p. e81841.
[43] Singer, E., Ishai, G., and Kimmel, E., 1995, "Parameter Estimation for a Prosthetic Ankle," Ann. Biomed. Eng., **23**(5), pp. 691–696.
[44] Pitkin, M. R., 2010, *Biomechanics of Lower Limb Prosthetics*, Springer Verlag, Berlin.
[45] ISO, 2016, "Prosthetics—Structural Testing of Lower-Limb Prostheses—Requirements and Test Methods," Standard No. ISO 10328:2016.
[46] Kadaba, M. P., Ramakrishnan, H. K., and Wootten, M. E., 1990, "Measurement of Lower-Extremity Kinematics During Level Walking," J. Orthop. Res., **8**(3), pp. 383–392.
[47] Hansen, A., 2008, "Effects of Alignment on the Roll-Over Shapes of Prosthetic Feet," Prosthetics Orthotics Int., **32**(4), pp. 390–402.
[48] Olesnavage, K. M., and Winter, A. G., 2016, "Design and Preliminary Testing of a Prototype for Evaluating Lower Leg Trajectory Error as an Optimization Metric for Prosthetic Feet," ASME Paper No. DETC2016-60565.
[49] Crimin, A., Mcgarry, A., Harris, E. J., and Solomonidis, S. E., 2014, "The Effect That Energy Storage and Return Feet Have on the Propulsion of the Body: A Pilot Study," J. Eng. Med., **228**(9), pp. 908–915.
[50] Snyder, R. D., Powers, C. M., Fontaine, C., and Perry, J., 1995, "The Effect of Five Prosthetic Feet on the Gait and Loading of the Sound Limb in Dysvascular Below-Knee Amputees," J. Rehabil. Res. Dev., **32**(4), pp. 309–315.
[51] Fukuchi, C. A., Fukuchi, R. K., and Duarte, M., 2018, "A Public Dataset of Overground and Treadmill Walking Kinematics and Kinetics in Healthy Individuals," PeerJ, **6**, p. e4640.
[52] Bovi, G., Rabuffetti, M., Mazzoleni, P., and Ferrarin, M., 2011, "A Multiple-Task Gait Analysis Approach: Kinematic, Kinetic and EMG Reference Data for Healthy Young and Adult Subjects," Gait Posture, **33**(1), pp. 6–13.

[53] Su, P. F., Gard, S. A., Lipschutz, R. D., and Kuiken, T. A., 2007, "Gait Characteristics of Persons With Bilateral Transtibial Amputations," J. Rehabil. Res. Dev., **44**(4), pp. 491–501.
[54] Glanzer, E. M., and Adamczyk, P. G., 2018, "Design and Validation of a Semi-Active Variable Stiffness Foot Prosthesis," IEEE Trans. Neural Syst. Rehabil. Eng., **26**(12), pp. 2351–2359.
[55] Adamczyk, P. G., Roland, M., and Hahn, M. E., 2017, "Sensitivity of Biomechanical Outcomes to Independent Variations of Hindfoot and Forefoot Stiffness in Foot Prostheses," Human Mov. Sci., **54**, pp. 154–171.
[56] Handford, M. L., and Srinivasan, M., 2016, "Robotic Lower Limb Prosthesis Design Through Simultaneous Computer Optimizations of Human and Prosthesis Costs," Sci. Rep., **6**(1), pp. 1–7.